Molecular Electronics

DOI: 10.1002/anie.201207116

Tactile-Feedback Stabilized Molecular Junctions for the Measurement of Molecular Conductance**

*I-Wen Peter Chen, Wei-Hsiang Tseng, Mong-Wen Gu, Li-Chen Su, Chan-Hsian Hsu, Wei-Hsuan Chang, and Chun-hsien Chen**

A fundamental understanding of the intrinsic properties of molecular electronics is expedited by the advancement of measurement devices[1] for single-molecule conductance. The most prevalent approaches are break-junction methods, such as mechanically controllable break junctions[2] and scanning tunneling microscopy (STM) break junctions,[3] which involve a pair of metal electrodes repeatedly being pushed towards each other and then pulled apart again. Such gaps have spacings momentarily suitable to host molecules. Other than a few exceptions,[4] this timescale is hundredths to tenths of a second, making it difficult to study time-dependent properties. Herein, we integrate an additional force-based control to adjust the junction spacing. Stable junctions on the order of minutes are possible and allow the study of single-molecule conductance from just one molecular junction, as opposed to those from collective data sets acquired on the millisecond timescale.[5]

Conductive atomic force microscopy (cAFM) is a powerful technique used to unravel the electrical properties of molecules using monolayers[6] and single molecules.[7–10] For monolayers pre-assembled on a metallic substrate, the positioning of the metal-coated AFM tip on the monolayers readily furnishes the metal-molecule-metal (MMM) configuration.[6] For single-molecule studies, gold nanoparticles are attached on alkanedithiols diluted in a slightly shorter monothiol matrix. The nanoparticle establishes the tip–molecule contact and hence, the measurements.[7] Note that, in these AFM-based methods, the tip exerts pressure on the molecules. Alternatively, the concept of STM break junctions is applicable to cAFM. Results of AFM break junctions are consistent with those of STM break junctions and show rupture forces of 1.5 nN,[8] 0.5 nN,[9] and 0.8 nN,[9,10] respectively, for Au-Au, Au-amino, and Au-pyridyl interactions. However, the study of *i*-V (current versus voltage) behavior remains difficult owing to the very short time span of the dynamic formation and rupture of molecular junctions.[11]

Herein, we have developed a new approach to make MMM junctions stable for multiple single-molecule *i*-V measurements or monitoring *i*(t) behavior. Instead of having a pre-programmed setting to move the tip back and forth monotonously at a constant speed, the positioning of the piezoelectric transducer is steered to maintain a constant tip-molecule force. To realize this method, we use herein a commercially available PicoAngler™ (MultiMode PicoForce, Veeco),[12] already proven valuable for single-molecule force spectroscopy, such as the study of mechanical unfolding of proteins or rupture forces.[13] The force-feedback feature allows the operator to experience the tactile feeling arising from the interaction between the tip and the sample. In response to the drift or change of the tip-molecule force, the piezoelectric scanner is manually adjusted to counteract the mechanical instability and thus to prolong the MMM junction.

The model compounds examined are alkanedithiols, the most studied molecules for creating MMM junctions, which can be easily configured owing to strong S-Au adsorption. The S-Au interaction is so strong that the stretching of the molecules may pull gold atoms out of the electrodes before the MMM junction breaks.[8,14] Multiple conductance maxima have been reported and attributed to preferential S-Au contact geometries.[15–18] For comparison, $Ph_2P(CH_2)_8PPh_2$ was studied because the P-Au adsorption is weaker than a Au-Au bond and because this compound has only one set of conductance values (i.e., no preferential anchoring site).[19,20] With stable molecular junctions, important issues include: 1) the correlation of molecular conductance with the applied force, for example, the stretched and relaxed conformations, and 2) the comparison of molecular conductance obtained from one single molecule in one junction with those from numerous MMM junctions.

To validate this new measurement technique, procedures similar to STM/AFM break junctions are used to compare the findings with published results. Figure 1 a,d displays, for α,ω-octanes, traces of force (F(t)) and conductance (G(t)). Positive or negative force regimes indicate, respectively, that the tip is pushed against or pulled away from the substrate. Hence, the portion of F(t) below the red dotted lines indicates that the tip is detached from the substrate and consequently that the molecule is stretched. F(t) traces show that the rupture forces needed to break the junctions are 1.29-(±0.28) nN for the cases of thiol and 0.66(±0.22) nN for biphenylphosphine, consistent with published values.[8,20] It is

[*] Prof. I-W. P. Chen[+]
Department of Applied Science, National Taitung University
Taitung, Taiwan 95002 (Taiwan)
Dr. W.-H. Tseng,[+] M.-W. Gu, Dr. L.-C. Su, C.-H. Hsu, W.-H. Chang, Prof. C.-h. Chen
Department of Chemistry and Center for Emerging Materials and Advanced Devices, National Taiwan University
Taipei, Taiwan 10617 (Taiwan)
E-mail: chhchen@ntu.edu.tw
[+] The authors contribute equally to this work.

[**] The authors thank NSC (Taiwan) and AOARD for the financial support. Thanks also to Prof. C.-M. Chiang (NSYSU), Dr. H.-B. Li, Dr. C.-T. Kou, F.-R. Tsai, and F.-M. Chen for the manuscript preparation.

Supporting information for this article is available on the WWW under http://dx.doi.org/10.1002/anie.201207116.

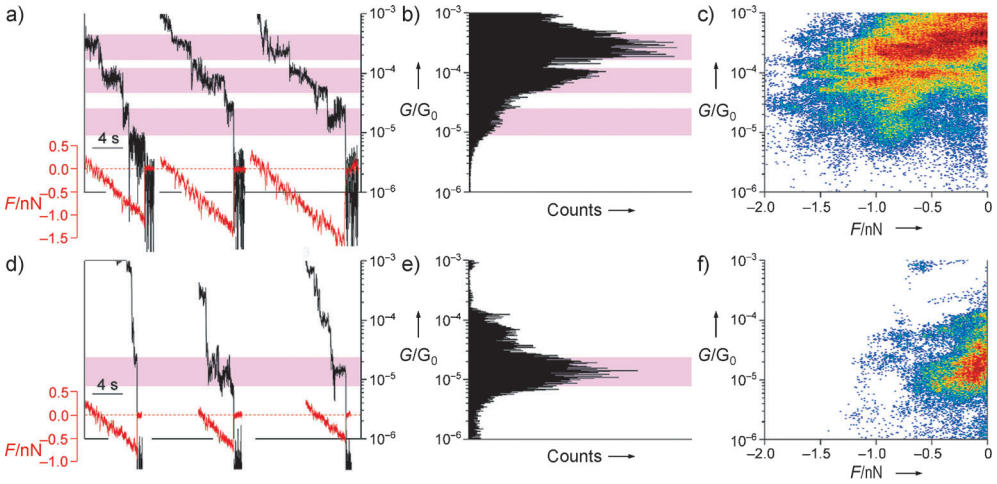

Figure 1. Conductance distributions of $HS(CH_2)_8SH$ (a–c) and $Ph_2P(CH_2)_8PPh_2$ (d–f). a,d) Force and conductance traces, b,e) conductance histograms, and c,f) conductance histograms plotted against force exerted on the MMM junction. The pink areas indicate the most probable conductance regimes. The conductance histograms are prepared from hundreds of traces without selection. Only the conductance data under pulling conditions, namely $F \leq 0$, appear in the histograms. Those with $F > 0$ would appear to the right hand side of the origin (see Figure S3) and are not displayed because the implication of the tip pressing on the substrate is too complicated. The logarithmical histograms are prepared using 100 bins per order of magnitude. Solutions: 1 mM α,ω-alkanes in toluene.

generally accepted that the rupture force for S-Au junctions arises from breaking Au-Au chains because the strength of the Au-Au bond is weaker and establishes the upper limit of the disruptive force.[8,21] In contrast, the breakage of Ph_2P-$(CH_2)_8PPh_2$ junctions likely takes place at Ph_2P-Au contact.[20] G(t) data with $F \leq 0$ nN are put together to generate conductance histograms with tip-pulling conditions (Figure 1 b,e) and plotted as a function of stretching force (Figure 1 c,f). Note that this is distinct from published reports in which the histograms were plotted against the tip displacement,[9,20,22] instead of against the force applied to the molecule.[20] Figure 1 b,e were prepared using all the traces obtained, that is, without subjective trace selection. After taking the logarithm of the raw data, 300 equal-sized bins are used to assemble the histograms. The results of $HS(CH_2)_8SH$ show multiple conductance peaks at $2.5(\pm0.6)\times10^{-4}$ G_0, $8.5(\pm1.7)\times10^{-5}$ G_0, and $1.5(\pm0.4)\times10^{-5}$ G_0 where G_0 is 77.5 μS, the conductance of quantum point contacts. For $Ph_2P(CH_2)_8PPh_2$, only one conductance peak is found, at $1.1(\pm0.4)\times10^{-5}$ G_0, consistent with previous STM/AFM break junction studies.[19,20] When the conductance histograms are drawn on a linear scale and the region of the distribution maxima is considered, peaks with integer multiples of the fundamental one are observed. The conductance values are thus determined (Supporting Information, Table S1). The number of counts is suppressed at the low-conductance regime (e.g., the peak at 1.5×10^{-5} G_0 in Figure 1 b) or relatively over-emphasized for high conductance peaks (e.g., around 2.5×10^{-4} G_0 in Figure 1 b). When the histogram of Figure 1 b is prepared by linear bins, the most prominent peak is not located at approximately 2.5×10^{-4} G_0, but at 1.1×10^{-5} G_0. This discrepancy has been discussed in the literature[23] (see Figure S1 and S2). The conductance values for $HS(CH_2)_6SH$ and $HS(CH_2)_{10}SH$ are summarized in Table S1.

Altogether, these results agree with the published values[15,16,24,25] and validate this new approach that limits the use of conductance data to the negative force regime. Those with the tips pushing against the substrate would be plotted at the positive side of the abscissa and are not displayed in Figure 1 because of its ambiguity about tip-molecule force (Figure S3). For the higher conductance maxima of 2.5×10^{-4} G_0 and 8.5×10^{-5} G_0, Figure 1 c shows that the relative occurrence of the fundamental peaks becomes prominent after the junction is stretched only a little (approximately −0.1 nN). *G*-*F* plots exhibit triangle-shaped occurrence (Figure S4), showing that the relative occurring frequencies for the integer multiples of the fundamental values decrease with the stretching force. Otherwise, the two conductance values are nearly force-independent. For the lowest conductance set, it requires a larger tip-molecule force (< -0.5 nN) to make apparent the occurring frequencies. In Figure 1 f, the occurrence of probable conductance for $Ph_2P(CH_2)_8PPh_2$ also resembles a right-angled triangle, with a narrower conductance distribution at a larger stretching force.

Figure 2 presents junctions stabilized by taking advantage of the good control over the tip-molecule force. The force traces show the degree of fluctuation that occurred when the

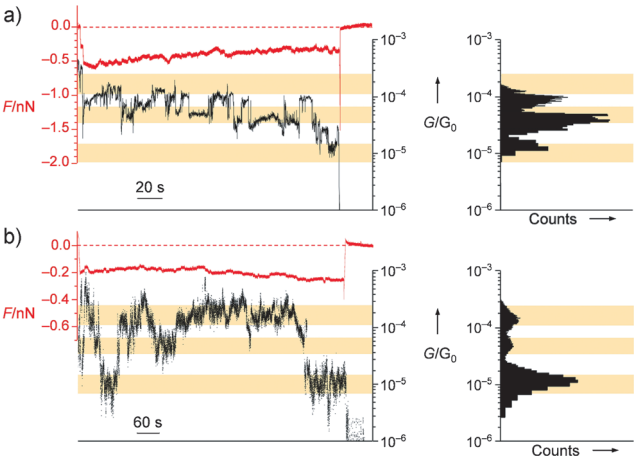

Figure 2. Traces of F(t) (red) and G(t) (black) and the corresponding conductance histograms (right) to demonstrate the stability of the Au-$HS(CH_2)_8SH$-Au junction. The concentrations of $HS(CH_2)_8SH$ were a) 1×10^{-3} M and b) 2×10^{-12} M. The dashed lines indicate the force baseline and the yellow areas represent the conductance regimes of the fundamental HC, MC, and LC peaks.

operator managed to keep the force at a certain value, that is −0.5 to −0.2 nN in the two examples. In Figure 2a, this junction was terminated deliberately to reveal the breaking force of −1.5 nN, corresponding to that of the Au-Au bond rupture. The force trace bounced directly back to the baseline without exhibiting a subsequent sawtooth feature (e.g., Figure 1a) and, prior to the end of the run, the conductance was consistent with those of the low conductance (LC) set, indicative of a junction with a very limited number of molecules. The conductance trace, $G(t)$, exhibited plateaus and resulted in multiple conductance peaks. However, some plateaus showed conductance around 1.0×10^{-4} G_0, smaller than that of high conductance (HC) and ascribable to a junction with two molecules adopting medium conductance (MC) configurations (also see Figure S4). To lower the events of having multiple molecules in the junction, the concentration of octanedithiol was diluted to 2 pM. Figure 2b shows a 12 minute run and the occurrence of the conductance being outside the regimes of the fundamental values is greatly reduced. In general, the molecular junctions lasted 300 s for $HS(CH_2)_8SH$ and 100 s for $Ph_2P(CH_2)_8PPh_2$. The acquisition of multiple *i*-V curves from the same junction becomes possible.

Figure 3 shows the stability of junctions formed in this manner for molecular *i*-V characterization. For visual comparison, Figure 3a and c are overlaid *i*-V curves for $HS(CH_2)_8SH$ obtained from one and 187 junctions, respectively.

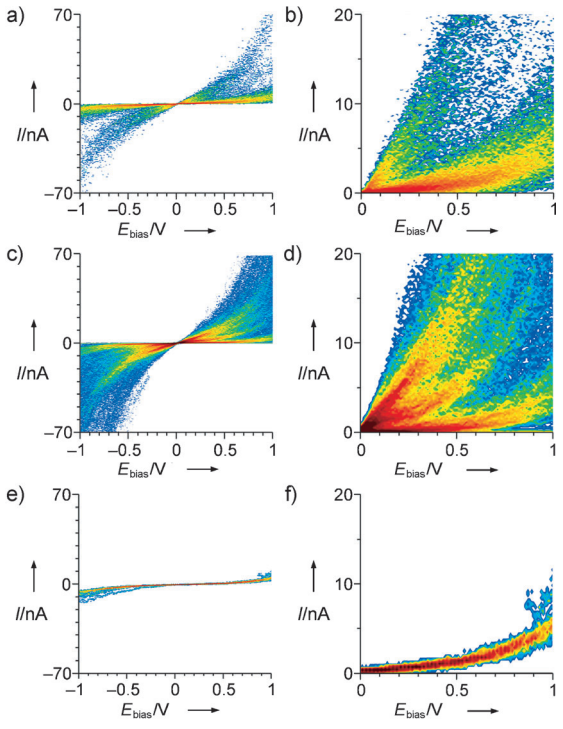

Figure 3. *i*-V characteristics obtained by a,b) one junction or c,d) hundreds of junctions for $HS(CH_2)_8SH$ and e,f) one junction for $Ph_2P(CH_2)_8PPh_2$. b,d,f) Magnified views of the left panels. a) 536 and e) 10 *i*-V traces under stretching forces of −0.8 (±0.2) nN and about −0.2 nN in the single-junction experiments. c,d) *i*-V graphs are plotted from 187 MMM junctions. Solutions: (a,b) 2 pM and (c–f) 1 mM α,ω-alkanes in toluene.

2 pM $HS(CH_2)_8SH$ was used for Figure 3a while 1 mM, more typically used in the field, was used for Figure 3c. On the right, magnifications of Figure 3a,c,e are shown. Figure 3b does not show MC curves for this particular junction. Figure 3d exhibits all three distinct groups yet includes additional features attributable to two molecules. Within the ohmic range used, the conductance values are about 1.5×10^{-4} G_0, 5.0×10^{-5} G_0, and 1.0×10^{-5} G_0, in reasonable agreement with those obtained by break junction methods (e.g., Figure 1b and Table S1).[15,16,24,25] The resemblance between Figure 3b and d confirms that the duration of a single junction is sufficiently long for such studies. In addition, their similarity and disparity illustrate the correlation between single-molecule *i*-V behaviors from a particular molecule in one MMM junction, versus from numerous junctions. Specifically, for individual molecules in a junction, *i*-V curves arbitrarily take place at three conductance domains, consistent with the $G(t)$ behavior shown in Figure 2. For the case of $Ph_2P(CH_2)_8PPh_2$ in one junction (Figure 3e,f), only one set of *i*-V curves is observed and the conductance value is centered at 1.0×10^{-5} G_0, using a bias of 0.1 V.

In an effort to explain the effect of tip-molecule force on the molecular conductance, Figure 4 was obtained with the applied force reversibly adjusted in a segmented manner for $HS(CH_2)_8SH$ and $Ph_2P(CH_2)_8PPh_2$ junctions. The magnitude

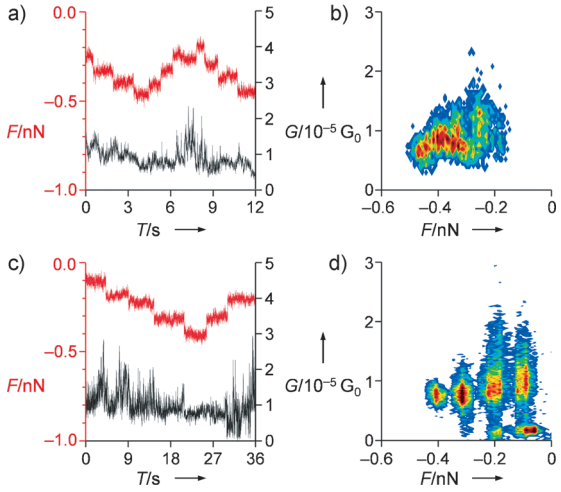

Figure 4. Conductance response as a function of applied force for a,b) $HS(CH_2)_8SH$ and c,d) $Ph_2P(CH_2)_8PPh_2$. To avoid complications to the data from stochastic changes in S-Au contact geometries, the presented traces are limited to those around 1×10^{-5} G_0.

of fluctuation in $G(t)$ appears associated with the applied force. By plotting the conductance against the applied force (Figure 4b,d), it is apparent that a stronger stretching force results in a narrower fluctuation in conductance.

We were unsure as to how to correlate the conductance with the molecular conformation by using the tip-stretching distance. A longer tip stretching renders a wider junction that straightens the bridged polymethylene chains. It would be reasonable to attribute the change in conductance to the transformation of α,ω-alkanes with *gauche* conformers into those with all-*trans* structures. However, previous reports

found contradictory conclusions about which of the conformers, *gauche* or *trans*, is more conductive.[16,18,25–28] The correlation is not straightforward because, besides the spacing of the junction, the distance the tip travels involves the sliding of gold atoms, because of the stronger S-Au bond than that of Au-Au interactions. Furthermore, the rapid forming and breaking up of the junction make it difficult to untangle the effect of conformational changes from factors that also affect the measured conductance, such as the preferential S-Au binding sites, continuous atomic-level restructuring at the site of contact, and the degree of deviation from the optimal bond lengths and C-S-Au angles at the contact before the rupture of the molecular junctions.

Using our setup, the MMM junctions can be stably maintained. The method shown in Figure 4 simplifies the data analysis, because the stretching tension does not reach an extreme and the G(t) trace does not jump between those ascribed to the contact geometries. These results show that a smaller stretching force yields a slightly larger conductance value accompanied by a larger fluctuation, which oscillates toward the more conductive side, instead of being symmetrically distributed. Assuming that the restructuring of contact geometries is not involved, our results suggest that the *gauche* conformers are only slightly more conductive than the *trans* conformers. This finding agrees with the experimental results of Nichols and co-workers[25,26] and with a modeling study by Jones and Troisi,[28] who proposed that the introduction of a single *gauche* conformation leads to lower conductance, yet multiple *gauche* defects create coupling between nonadjacent methylene units and confer a through-space pathway more efficient than that of the all-*trans* conformer.

In conclusion, a tactile-feedback controlled conductive AFM was used to generate minute-long MMM junctions. The pulling feature allows the molecular conductance to be scrutinized as a function of the tip-molecule force. A stronger stretching force leads to an increase of the occurring frequencies for the fundamental conductance relative to those of the integer multiples, while the conductance values decrease only slightly. Minute-long G(t) traces show molecular conductance toggling spontaneously between those ascribed to preferential S-Au contact geometries. The acquisition of hundreds of *i*-V curves in one MMM junction is possible and shows three groups of *i*-V traces for HS-$(CH_2)_8$SH and one group for $Ph_2P(CH_2)_8PPh_2$. Finally, by holding the MMM junction at one preferential S-Au contact geometry, the correlation of the tip-molecule force with the conductance fluctuation suggests that *gauche* conformers are slightly more conductive than *trans* conformers. Through the superior sensitivity to force, this tactile-feedback controlled cAFM offers new opportunities to study systems that require no destruction to the electrodes, such as, different electrode materials for the tip and substrate.

Experimental Section

AFM break junctions were carried out in a toluene-filled fluidic cell (MTFML, Bruker) and a NanoscopeIIIa controller (Veeco). An external source/measure unit (B1500A, Agilent) was used to improve the available current range to 0.1 mA–10 pA. For the commonly used AFM break junction, the tip was loaded against the substrate until the current reached a pre-set value of 0.1 mA at an E_{bias} around 0.1–0.2 V, equivalent to 0.5–1 mS or 6–13 G_0. The tip was subsequently pulled away from the substrate at a constant speed, typically 0.6–10 $nm\,s^{-1}$. Another method was developed herein to obtain molecular junctions stable for minutes. The deformation of the piezoelectric scanner was adjusted manually by a real-time tactile-feedback device (PicoAngler™, Veeco) in which, using the torque exerted on a knob, the operator experienced the tip-sample force and tuned the tip position to maintain the junction. To minimize the effect of mechanical drift, the measurements were performed at least 4 hours after the system was assembled.

Received: September 3, 2012
Revised: December 5, 2012
Published online: January 22, 2013

Keywords: alkanedithiols · charge transfer · conductive atomic force microscopy · molecular electronics · molecular junctions

[1] a) H. Song, M. A. Reed, T. Lee, *Adv. Mater.* **2011**, *23*, 1583–1608; b) M. Tsutsui, M. Taniguchi, *Sensors* **2012**, *12*, 7259–7298.
[2] M. A. Reed, C. Zhou, C. J. Muller, T. P. Burgin, J. M. Tour, *Science* **1997**, *278*, 252–254.
[3] B. Xu, N. J. Tao, *Science* **2003**, *301*, 1221–1223.
[4] a) W. Lee, P. Reddy, *Nanotechnology* **2011**, *22*, 485703; b) M. L. Perrin, F. Prins, C. A. Martin, A. J. Shaikh, R. Eelkema, J. H. van Esch, T. Briza, R. Kaplanek, V. Kral, J. M. van Ruitenbeek, H. S. J. van der Zant, D. Dulić, *Angew. Chem.* **2011**, *123*, 11419–11422; *Angew. Chem. Int. Ed.* **2011**, *50*, 11223–11226; c) D. Dulić, F. Pump, S. Campidelli, P. Lavie, G. Cuniberti, A. Filoramo, *Angew. Chem.* **2009**, *121*, 8423–8426; *Angew. Chem. Int. Ed.* **2009**, *48*, 8273–8276; d) Z. Liu, S.-Y. Ding, Z.-B. Chen, X. Wang, J.-H. Tian, J. R. Anema, X.-S. Zhou, D.-Y. Wu, B.-W. Mao, X. Xu, B. Ren, Z.-Q. Tian, *Nat. Commun.* **2011**, *2*, 305.
[5] Z. Huang, F. Chen, P. A. Bennett, N. Tao, *J. Am. Chem. Soc.* **2007**, *129*, 13225–13231.
[6] a) G. Wang, T.-W. Kim, T. Lee, *J. Mater. Chem.* **2011**, *21*, 18117–18136; b) L. Luo, S. H. Choi, C. D. Frisbie, *Chem. Mater.* **2011**, *23*, 631–645.
[7] a) T. Morita, S. Lindsay, *J. Am. Chem. Soc.* **2007**, *129*, 7262–7263; b) X. D. Cui, et al., *Science* **2001**, *294*, 571–574; c) I-W. P. Chen, M.-D. Fu, W.-H. Tseng, J.-Y. Yu, S.-H. Wu, C.-J. Ku, C.-h. Chen, S.-M. Peng, *Angew. Chem.* **2006**, *118*, 5946–5950; *Angew. Chem. Int. Ed.* **2006**, *45*, 5814–5818; d) D. S. Seferos, A. S. Blum, J. G. Kushmerick, G. C. Bazan, *J. Am. Chem. Soc.* **2006**, *128*, 11260–11267; e) H. Cohen, C. Nogues, R. Naaman, D. Porath, *Proc. Natl. Acad. Sci. USA* **2005**, *102*, 11589–11593.
[8] a) B. Xu, X. Xiao, N. J. Tao, *J. Am. Chem. Soc.* **2003**, *125*, 16164–16165; b) C. Nef, P. L. T. M. Frederix, J. Brunner, C. Schonenberger, M. Calame, *Nanotechnology* **2012**, *23*, 365201.
[9] M. Frei, S. V. Aradhya, M. Koentopp, M. S. Hybertsen, L. Venkataraman, *Nano Lett.* **2011**, *11*, 1518–1523.
[10] I. V. Pobelov, G. Mészáros, K. Yoshida, A. Mishchenko, M. Gulcur, M. R. Bryce, T. Wandlowski, *J. Phys. Condens. Matter* **2012**, *24*, 164210.
[11] a) E. Lörtscher, H. B. Weber, H. Riel, *Phys. Rev. Lett.* **2007**, *98*, 176807; b) C. A. Martin, D. Ding, H. S. J. van der Zant, J. M. van Ruitenbeek, *New J. Phys.* **2008**, *10*, 065008.
[12] a) Q. Zhang, J. Jaroniec, G. Lee, P. E. Marszalek, *Angew. Chem.* **2005**, *117*, 2783–2787; *Angew. Chem. Int. Ed.* **2005**, *44*, 2723–2727; b) G. Francius, S. Lebeer, D. Alsteens, L. Wildling, H. J. Gruber, P. Hols, S. De Keersmaecker, J. Vanderleyden, Y. F. Dufrene, *ACS Nano* **2008**, *2*, 1921–1929; c) H. Lu, W. Nowak, G.

Lee, P. E. Marszalek, W. Yang, *J. Am. Chem. Soc.* **2004**, *126*, 9033 – 9041.
[13] a) M. Rief, M. Gautel, F. Oesterhelt, J. M. Fernandez, H. E. Gaub, *Science* **1997**, *276*, 1109 – 1112; b) M. Rief, F. Oesterhelt, B. Heymann, H. E. Gaub, *Science* **1997**, *275*, 1295 – 1297.
[14] Y. Kim, T. J. Hellmuth, M. Bürkle, F. Pauly, E. Scheer, *ACS Nano* **2011**, *5*, 4104 – 4111.
[15] a) X. Li, J. He, J. Hihath, B. Xu, S. M. Lindsay, N. Tao, *J. Am. Chem. Soc.* **2006**, *128*, 2135 – 2141; b) W. Haiss, S. Martín, E. Leary, H. van Zalinge, S. J. Higgins, L. Bouffier, R. J. Nichols, *J. Phys. Chem. C* **2009**, *113*, 5823 – 5833.
[16] C. Li, I. Pobelov, T. Wandlowski, A. Bagrets, A. Arnold, F. Evers, *J. Am. Chem. Soc.* **2008**, *130*, 318 – 326.
[17] M. T. González, S. Wu, R. Huber, S. J. van der Molen, C. Schönenberger, M. Calame, *Nano Lett.* **2006**, *6*, 2238 – 2242.
[18] Y. Kim, H. Song, F. Strigl, H.-F. Pernau, T. Lee, E. Scheer, *Phys. Rev. Lett.* **2011**, *106*, 196804.
[19] R. Parameswaran, J. R. Widawsky, H. Vázquez, Y. S. Park, B. M. Boardman, C. Nuckolls, M. L. Steigerwald, M. S. Hybertsen, L. Venkataraman, *J. Phys. Chem. Lett.* **2010**, *1*, 2114 – 2119.
[20] M. Frei, S. V. Aradhya, M. S. Hybertsen, L. Venkataraman, *J. Am. Chem. Soc.* **2012**, *134*, 4003 – 4006.
[21] a) G. Rubio-Bolliger, S. R. Bahn, N. Agraït, K. W. Jacobsen, S. Vieira, *Phys. Rev. Lett.* **2001**, *87*, 026101; b) J. A. M. Sondag-Huethorst, C. Schonenberger, L. G. J. Fokkink, *J. Phys. Chem.* **1994**, *98*, 6826 – 6834.
[22] In the literature, the distance of elongation was derived from the piezoelectric movement of the tip after the breaking of gold atom chains, namely, a sharp conductance drop when G(t) became significantly smaller than 1 G_0. However, the tip sometimes was in the positive force regime and pushed against the substrate with the gold coating being worn out and the apex being nonconductive. The molecule-tip contact was bridged at the circumference of the remnant gold film, rather than at the apex. In addition, the elongation of the MMM junction involved dragging gold atoms and reshaping the electrodes. Therefore, operating under the positive force regime, the force applied to the molecules cannot be easily extracted from the AFM instrument and cannot be obtained by multiplying elongation distance with the force constant of the cantilever.
[23] R. Huber, et al., *J. Am. Chem. Soc.* **2008**, *130*, 1080 – 1084.
[24] a) M. T. González, J. Brunner, R. Huber, S. Wu, C. Schönenberger, M. Calame, *New J. Phys.* **2008**, *10*, 065018; b) C.-H. Ko, M.-J. Huang, M.-D. Fu, C.-h. Chen, *J. Am. Chem. Soc.* **2010**, *132*, 756 – 764; c) S. Guo, J. Hihath, I. Díez-Pérez, N. Tao, *J. Am. Chem. Soc.* **2011**, *133*, 19189 – 19197; d) M.-D. Fu, I-W. P. Chen, H.-C. Lu, C.-T. Kuo, W.-H. Tseng, C.-h. Chen, *J. Phys. Chem. C* **2007**, *111*, 11450 – 11455.
[25] S. Martín, W. Haiss, S. Higgins, P. Cea, M. C. López, R. J. Nichols, *J. Phys. Chem. C* **2008**, *112*, 3941 – 3948.
[26] W. Haiss, H. van Zalinge, D. Bethell, J. Ulstrup, D. J. Schiffrin, R. J. Nichols, *Faraday Discuss.* **2006**, *131*, 253 – 264.
[27] a) M. Fujihira, M. Suzuki, S. Fujii, A. Nishikawa, *Phys. Chem. Chem. Phys.* **2006**, *8*, 3876 – 3884; b) M. Paulsson, C. Krag, T. Frederiksen, M. Brandbyge, *Nano Lett.* **2009**, *9*, 117 – 121.
[28] D. R. Jones, A. Troisi, *J. Phys. Chem. C* **2007**, *111*, 14567 – 14573.

